J. Mt. Sci. (2016) 13(9): 1515-1526 e-mail: jms@imde.ac.cn http://jms.imde.ac.cn
DOI: 10.1007/s11629-016-3918-2

Three-dimensional stability of landslides based on local safety factor

YANG Tao[1,2] http://orcid.org/0000-0001-5072-7089; e-mail: yangtao@home.swjtu.edu.cn

Man-chu Ronald YEUNG[3] http://orcid.org/0000-0003-1011-0409; e-mail: mryeung@cpp.edu

YANG Bing[1,2*] http://orcid.org/0000-0002-4098-1419; e-mail: yangb@home.swjtu.edu.cn

LIU Yong-jiang[4] http://orcid.org/0000-0001-5072-7089; e-mail: liuyongjiang@cmhk.com

YANG Yan-xin[1] http://orcid.org/0000-0001-5072-7089; e-mail: actor99yyx@my.swjtu.edu.cn

** Corresponding author*

1 School of Civil Engineering, Southwest Jiaotong University, Chengdu 610031, China

2 MOE Key Laboratory of Transportation Tunnel Engineering, Chengdu 610031, China

3 Department of Civil Engineering, California State Polytechnic University, Pomona, CA 91768, USA

4 Transportation Research Institute of Chongqing, Chongqing 400072, China

Citation: Yang T, Yeung MC, Yang B, et al. (2016) Three-dimensional stability of landslides based on local safety factor. Journal of Mountain Science 13(9). DOI: 10.1007/s11629-016-3918-2

Abstract: Unlike the limit equilibrium method (LEM), with which only the global safety factor of the landslide can be calculated, a local safety factor (LSF) method is proposed to evaluate the stability of different sections of a landslide in this paper. Based on three-dimensional (3D) numerical simulation results, the local safety factor is defined as the ratio of the shear strength of the soil at an element on the slip zone to the shear stress parallel to the sliding direction at that element. The global safety factor of the landslide is defined as the weighted average of all local safety factors based on the area of the slip surface. Some example analyses show that the results computed by the LSF method agree well with those calculated by the General Limit Equilibrium (GLE) method in two-dimensional (2D) models and the distribution of the LSF in the 3D slip zone is consistent with that indicated by the observed deformation pattern of an actual landslide in China.

Received: 2 March 2016
Revised: 13 May 2016
Accepted: 2 June 2016

Keywords: Landslide stability; Local safety factor; Stability analysis method; Slip mechanism

Introduction

Landslides occur in many parts of the world every year. Large landslides lead to severe damages to the environment and even life loss (Jaeger 1965; Werner and Friedman 2010). The stability and sliding mechanisms of landslides have attracted interest of many researchers (Alemdag et al. 2014; 2015; Kaya et al. 2016; Jaiswal et al. 2011).

Limit equilibrium methods (LEMs) have been widely adopted for landslide stability analyses mainly due to the simplicity that the methods offer (Morgenstern and Price 1965, 1967; Duncan 1996; Ozbay and Cabalar 2015). This is usually reasonable because the results from 2D analyses are usually on the safe side. Sometimes the safety factor nomograms was used to evaluate the stability of homogeneous earth dams (Mendoza et al. 2009). Slip surfaces of all landslides, however, take on three-dimensional (3D) forms in reality (Xu 2011). Therefore, 3D analyses have gained increasing attention.

Some procedures that consider the effects of the third dimension were developed through extending their 2D counterparts. Baligh and Azzouz (1975) and Chen and Chameau (1982) considered the slip surface of a cylinder of finite length with either cones or ellipsoids attached to its ends, based on the ordinary method of slices. Anagnosti (1969) extended the general method proposed by Morgenstern and Price (1965). These methods satisfy only part of the equilibrium conditions under the assumption that the failure mass has a symmetrical plane so as to eliminate the static indeterminate condition. Huang and Tsai (2002) proposed a 3D LEM, which satisfies "two force and one moment equilibrium conditions" with slip surfaces of arbitrary shapes. In the procedure presented by Leshchinsky and Huang (1992), three force equilibrium conditions and one moment equilibrium condition about a rotation axis are satisfied, and the equilibrium equations are formulated from the entire sliding mass instead of individual slices. Another basic fact is that almost all existing LEMs, neither methods of 2D nor methods of 3D are able to in advance generate a system of forces that satisfies the reasonable conditions suggested by Morgenstern and Price (1965).

Krahn (2003) discussed the limitation of the LEM, and they pointed out that the LEM does not consider strain and displacement compatibility. This has two serious consequences. One is that local variations in safety factors cannot be considered, and the second is that the computed stress distributions are often unrealistic. In fact, a landslide always has different displacements or levels of stability at different parts. This means that different parts of the slip surface have different local safety factors, with major implications as to the failure mechanism of the landslide.

The local safety factor proposed by Ono (1962) or stress severity (inverse of the local safety factor) as proposed by Fairhurst (1964) is commonly used to quantify the stability at any point of a structure. The local safety factor is usually dependent on the failure criterion. Okubo et al. (1997) proposed a modified local safety factor to extend its application to most failure criteria. Srbulov (1987) and Wang (1982) adopted a local safety factor to analyze the stability of a rock mass, and it is defined as:

$$F_s = \frac{\sigma_c}{\sigma} \tag{1}$$

where σ_c is the strength of the rock mass, and σ is the stress in the rock mass. Obviously, this definition does not take the actual slip surface of the landslide into account. As a result, it is only appropriate for judging the stability of a rock mass.

Hoek and Bray (1981) introduced the concept of local safety factor in the analysis of slope stability. The definition of local safety factor is the ratio of the maximal shear strength and the effective shear stress on the slip surface. Using Mohr-Coulomb criterion, for example, the local safety factor can be calculated as:

$$F_s = \frac{c\cos\varphi + \frac{\sigma_1+\sigma_3}{2}\sin\varphi}{\frac{\sigma_1-\sigma_3}{2}} \tag{2}$$

where c and φ are the cohesion and internal friction angle, respectively; and σ_1, σ_3 are the major and minor principal stresses, respectively. From Equation (2), we also can see that, the slip surface is just the shear failure surface corresponding to the given stress state; it is not the actual slip surface of the landslide. This local safety factor is also a kind of strength factor.

For a 3D wedge slope, Yao et al. (1984) gave a definition of local safety factor (η) based on the normal stress (σ_n) and the maximum shear stress (τ_{max}) on the slip surface for the case of an existing slip surface:

$$\eta = \frac{\sigma_n \tan\varphi + c}{\tau_{max}} \tag{3}$$

This definition can be used to analyze a landslide having a simple planar slip surface. For a landslide with a 3D complex slip surface, the direction normal to the slip surface varies. Generally speaking, the sliding direction varies along the slip surface. Therefore, the variations of the normal direction and sliding direction of the slip surface must be considered to arrive at a reasonable definition of the local safety factor.

Because landslides always have different spatial shape, it is more reasonable for investigation of landslide stability with 3-D analysis method. However, mature and simple methods in three-dimension are still not available at present (Zheng 2012). Therefore, it is necessary to define a physical parameter to quantify the sliding mechanism of the landslide and to indicate the stability of the landslide.

In this study a novel definition of safety factor is proposed. The normal stress and shear stress are calculated according to the local direction normal to the slip surface. And the shear stress is decomposed into sliding shear stress along the sliding direction. The local safety factor is calculated according to the normal stress and the sliding shear stress. The global safety factor of the landslide is also defined and discussed according the weighted average of local safety factors based on the slip surface area. Thus the spatial failure mechanism of the landslide can be evaluated by analyzing the distribution of local safety factors calculated for elements of slip zones.

1 Determination of Element Stress in Slip Zone

The slip surface of the landslide can be localized by many methods. Hutchinson (1982) reviewed the main methods of discovering the shape and locating the slip surface in landslides after stressing the importance of surveying. Baker (1980), Nguyen (1985) and Kahatadeniya (2009) used optimization-based techniques to search for the critical slip surface in the slope stability analysis. Mankelow (1998) and Van (1994) conducted a GIS-based method for locating the critical slip surface in slope. When the slip surface of the landslide is known, the calculation model of the landslide can be established and the local safety factor can be calculated.

The determination of the local safety factor in the slip zone depends on the stress state in the slip zone. Therefore, the stress state of the slip zone must be obtained first, through 3D numerical simulations. In this paper, the stress field of the landslide is calculated by FLAC3D. In a numerical model, the slip zone is discretized into thin elements (i.e. the size of the element (d) along the normal direction of slip zone is small). The elements in the slip zone have been discretized as thinly as possible if the compatibility of the elements' sizes would meet the necessary requirements of the numerical model. The size of the element (l) in the tangential direction is set to be much larger than that in the normal direction (d) (usually $l > 3d$) so that the normal vector of the slip element can be precisely determined.

A landslide can be divided into three zones: the slip mass, slip zone, and the slip bed (Hoek and Bray 1981). The constitutive relation of the material of the slip mass can be selected as nonlinear so as to be compatible with the nature of the rock-soil body. The slip bed is static during the failure of the landslide, and the constitutive relation of the slip bed can simply be an elastic model. The Mohr-Coulomb criterion is adopted for the elements of the slip zone.

The procedure of stress state calculation can be divided into three steps. The first step is that the initial stress field of the global slope is obtained with the elastic constitutive model, and the second step is that the true stress field of the slope is obtained with the constitutive model corresponding to the practical material of the slope. The third step is that the displacement increment of the element node of the slip zone is determined from the results in the first and second steps. With these three steps, the true stress states of the elements and the true sliding directions of the nodes in the slip zone can be obtained. Therefore, the local safety factor of the element in the slip zone and the global safety factor of the landslide can be computed.

2 Determination of Local Safety Factor of Element in Slip Zone

2.1 Normal and tangential vector of a slip surface

The slip zone is discretized by thin eight-node hexahedral elements. The long side of the element is parallel to the slip zone, and the short side is perpendicular to the slip zone. The node numbers of an eight-node hexahedral element are shown in Figure 1. The coordinates of the nodes are set as x_i, y_i, z_i (i=1~8). Thus, the coordinates of the mid-point of the short side of the element $P_{1,4}, P_{2,7}, P_{3,6}, P_{5,8}$ can be easily obtained (FLAC3D 2005). For example, the coordinates of the mid-point of the side 1-4 can be written as $P_{1,4}^x, P_{1,4}^y, P_{1,4}^z$.

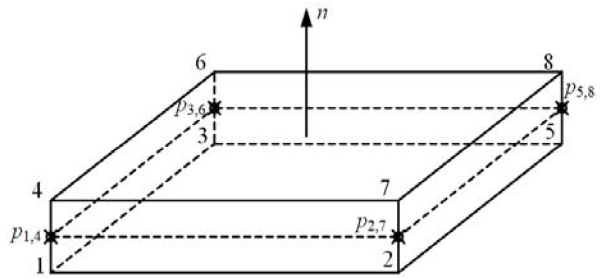

Figure 1 Node numbering of the element in the slip zone.

It is shown in Figure 1 that the cross product of vector $P_{1,4}, P_{2,7}$ and vector $P_{1,4}, P_{3,6}$ is the normal vector of the slip surface, which passes through the center of the element, and it can be written as

$$\mathbf{N}=\overrightarrow{P_{1,4}P_{2,7}}\times\overrightarrow{P_{1,4}P_{3,6}}$$

$$=\begin{vmatrix} i & j & k \\ P_{2,7}^{x}-P_{1,4}^{x} & P_{2,7}^{y}-P_{1,4}^{y} & P_{2,7}^{z}-P_{1,4}^{z} \\ P_{3,6}^{x}-P_{1,4}^{x} & P_{3,6}^{y}-P_{1,4}^{y} & P_{3,6}^{z}-P_{1,4}^{z} \end{vmatrix} \quad (4)$$

The displacement vector of the element center can be written as

$$\left\{v_x=\frac{1}{8}\sum_{i=1}^{8}u_x^i, v_y=\frac{1}{8}\sum_{i=1}^{8}u_y^i, v_{xz}=\frac{1}{8}\sum_{i=1}^{8}u_z^i\right\} \quad (5)$$

where u_x^i, u_y^i, u_z^i are respectively the displacement component of the i^{th} node along the x-, y-, and z-direction.

The projection of the displacement vector of the element center, s, projected onto the plane $P_{1,4}, P_{2,7}, P_{3,6}$ is the slip direction of the element, namely,

$$s=(n\times v)\times n \quad (6)$$

The components of the vector, s, are

$$\begin{cases} s_x=(n_z v_x-n_x v_z)n_z-(n_x v_y-n_y v_x)n_y \\ s_y=(n_x v_y-n_y v_x)n_x-(n_y v_z-n_z v_y)n_z \\ s_z=(n_y v_z-n_z v_y)n_y-(n_z v_x-n_x v_z)n_x \end{cases} \quad (7)$$

The area of the triangle $p_{1,4}p_{2,7}p_{3,6}$ can be calculated from the coordinates of points $P_{1,4}, P_{2,7}, P_{3,6}$

$$S_{\Delta P_{1,4}P_{2,7}P_{3,6}}=\frac{1}{2}\left|\overrightarrow{P_{1,4}P_{2.7}}, \overrightarrow{P_{1,4}P_{3,6}}\right| \quad (8)$$

Similarly, the area of triangle $\Delta P_{5,8}P_{2,7}P_{3,6}$, can also be calculated. And thus the area of the slip zone represented by an element can be obtained by summing the area of triangles $\Delta P_{1,4}P_{2,7}P_{3,6}$ and $\Delta P_{5,8}P_{2,7}P_{3,6}$, i.e.

$$S_E=S_{\Delta P_{1,4}P_{2,7}P_{3,6}}+S_{\Delta P_{5,8}P_{2,7}P_{3,6}} \quad (9)$$

2.2 Normal and tangential stress on slip surface

As shown in Figure 2, point A is the center of an element, and the six stress components $\sigma_x\sigma_y, \sigma_z, \tau_x, \tau_y, \tau_z$, are known (Irons 1971). The relationship between the components of the normal stress in any inclined cross section passing through point A and the six stress components at point A is as follows:

$$\begin{Bmatrix} P_{nx} \\ P_{ny} \\ P_{nz} \end{Bmatrix}=\begin{bmatrix} \sigma_x & \tau_{yx} & \tau_{zx} \\ \tau_{xy} & \sigma_y & \tau_{zy} \\ \tau_{xz} & \tau_{yz} & \sigma_z \end{bmatrix} \quad (10)$$

where P_{nx}, P_{ny}, and P_{nz} are the components of the normal stress in the inclined cross section relative to the given coordinates; l, m, n are the direction cosines of the normal vector ($\vec{N}$) of the inclined cross section BCD relative to the coordinate axes x, y, z.

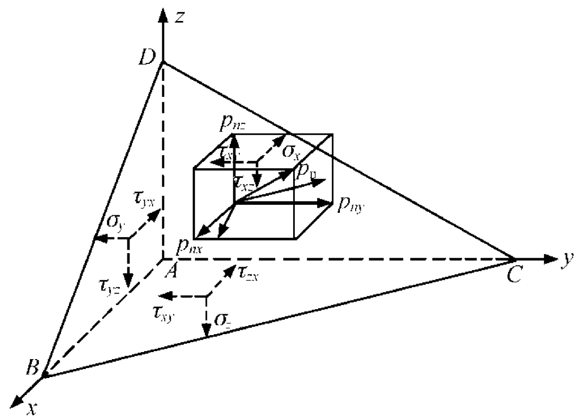

Figure 2 Stress status of space point.

The normal stress on the inclined cross section σ_n is

$$\sigma_n=p_{nx}l+p_{ny}m+p_{nz}n \quad (11)$$

The normal vector of the slip surface represented by Eq. (4) can be normalized and assumed as the following:

$$l=n_x m=n_y, n=n_z \quad (12)$$

where n_x, n_y, n_z are the components of the vector n in the x-, y- and z-direction, respectively. If Eq. (12) is substituted into Eq. (11), then the normal stress of the element (normal stress of the slip surface, σ_n), can be obtained. Similarly, the vector (Eq. 7) along the direction of the sliding of the element is normalized, and assumed as the following:

$$l = s_x, m = s_y, n = s_z \tag{13}$$

where s_x, s_y, s_z are the components of the vector s in the x-, y-, and z-direction, respectively. Eq. (13) is substituted into Eq. (11), then the tangential stress of the element (tangential stress of the slip surface,τ), can be obtained.

2.3 Definition of local safety factor

In numerical simulations, the occurrence of plastic yielding in one element in the slip zone only shows that the compressive stress and the maximum shear stress on the most dangerous cross section (shear failure plane) at this element meet the yield criterion. But the shear failure plane is not the same as the sliding surface; therefore, the compressive stress is not necessarily perpendicular to the sliding surface at that point. Even if the compressive stress is perpendicular to the sliding surface (that means the shear failure plane is the same as the sliding surface at that point), it cannot be certain that the maximum shear stress is along the direction of sliding. So the shear plastic yielding at one point in a slip zone does not mean that the normal stress perpendicular to the sliding surface and the shear stress parallel to the sliding direction meet the yield criterion at this point. Any element in the slip zone would be subject to the constraint of adjacent elements, and its deformation needs to meet the compatibility conditions. As a result, even though all the elements in the slip zone have been in the state of plastic yield, it does not mean that the global safety factor of the landslide is equal to 1.0 or that the landslide will be unstable. Only when all the normal stresses perpendicular to the slip zone and the shear stresses parallel to the sliding directions have met the yield conditions, the landslide would be unstable. This is also the reason why computational results still converge in the numerical analysis even when the elements in a slip zone have been completely in the state of plastic yield in FLAC3D.

The shear strength along the sliding direction at one point can be determined by

$$\tau_u = c + \sigma_n \tan \emptyset \tag{14}$$

where σ_n is the normal stress perpendicular to the slip surface calculated by Eq. (11); c is the cohesion; and $\emptyset$ is the internal friction angle.

The safety factor of one element in a slip surface is defined as

$$F_{se} = \frac{\tau_u}{\tau} \tag{15}$$

where τ is the shear stress in the sliding direction at this point, which can be determined by Eq.(13) and Eq. (11).

The global safety factor of the landslide is defined as

$$F_s = \frac{\sum_{i=1}^{ne} F_{se}^i S_E}{\sum_{i=1}^{ne} S_E^i} \tag{16}$$

where ne is the number of elements in the slip zone; F_{se}^i is the local safety factor of element i; and S_E^i is the area of the slip surface represented by element i , which is calculated by Eq. (9).

The stress field of a slope can be obtained through numerical simulation in which an appropriate constitutive model should be prudently selected. The elastic-perfectly plastic constitutive model based on the Mohr-Coulomb strength criterion is the most appropriate in geotechnical engineering, which is also suitable for the simulation of the rock-soil body of the slip zone in a landslide. Some hexahedral elements are adopted to discretize the slip zone. And the cross section i.e. middle cross section parallel to the slid surface, is a plane, on which the normal stress is the true normal stress at this point. In the computation process, there is a plastic deformation in the slip zone, and the direction of the element displacement vector represents the true sliding direction. The projection of the element displacement vector in the middle cross section is the true direction of the shear stress. Therefore, it is reasonable to adopt the Mohr-Coulomb strength criterion to define the safety factor of the element centroid. The safety factor at different element is no longer uniform due to the varying element stress state in the slip zone. The influence of different elements on the global safety factor depends on the corresponding area of slip zone represented by each element. Thus the global safety factor can be evaluated through the weighted average of the local safety factor based on the area of slip surface. It can be seen that the safety factor computed by Eq. (15) and Eq. (16) is the true evaluation of the stability of the slip zone without too many assumptions. From the calculated local safety factors, the stability of different parts of the slip zone can be judged, and furthermore, the failure mechanism of the landslide in 3D can be evaluated, which will be helpful in the design of landslide mitigation measures.

3 Validity of Local Safety Factor Method

A quasithreedimensional slope model, shown in Figure 3, is considered to verify the reliability of the local safety factor (LSF) method. The computational parameters are listed in Tables 1 and 2. There are four values for every parameter in Table 2. The value with an asterisk is the basic one. The parameters are changed based on the basic one for every computation. When one group of parameters are selected from Table 2, the cohesion and internal friction angle of the slip zone is selected from Table 1. Thus, there are sixteen combinations of parameters according to Table 1. Both the LSF and GLE methods are used to compute the safety factor of the slope based on these sixteen combinations of parameters.

The calculated results using the LSF method agree very well with the results using the GLE method. For example, when the slip mass is assigned different elastic moduli, Table 3 and Figure 4 show the calculated results. The global factor of safety is plotted against the combination of shear strength parameters in the slip zone in Figure 4. A curve represents a series of calculated results when the slip zone is assigned different shear strength parameters according to Table 1. These four curves are very close to each other; they look like just one curve. This means even the slip mass is assigned different elastic moduli in the numerical simulation, and the global factor of safety calculated by Eq.(16) is almost the same as that calculated by the GLE method.

The correlation coefficient can be calculated to describe the correlation between the LSF and GLE results. Table 4 presents the correlation coefficients of the two results computed respectively by the LSF and GLE methods. It can be seen from the table that all of the correlation coefficients are larger than 0.988, which means the results from the LSF and GLE methods are very close. While the global factor of safety is almost exclusively controlled by the shear strength parameters of the slip zone, the other calculation parameters will affect the distribution of the local safety factor.

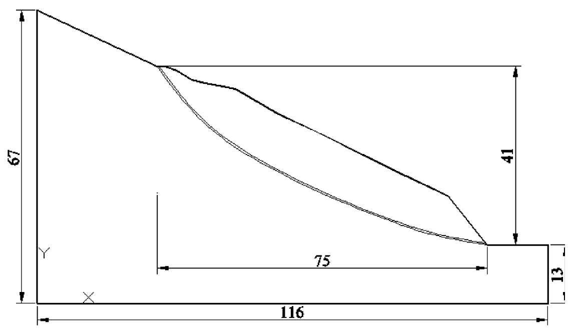

Figure 3 Diagram for 2D computational model (m).

Table 1 Shear Strength Parameter of Slip Zone

Parameter	Range			
c_Z (kPa)	65	50*	35	25
φ_Z (°)	32	28*	24	20

Notes: c_Z = Cohesion in slip zone; φ_Z = Internal friction angel in slip zone.

Table 2 Parameter Lever

Parameter	Value lever			
	1	2	3	4
E_B (MPa)	5000	1000*	500	50
μ_B	0.35	0.3	0.25*	0.2
c_B (kPa)	200*	150	100	60
φ_B (°)	30*	25	20	15
E_M (MPa)	160	80*	40	20
μ_M	0.38	0.3*	0.25	0.2
c_M (kPa)	80*	50	35	25
φ_M (°)	20*	10	8	4
E_Z (MPa)	100	60	30*	10
μ_Z	0.4	0.35*	0.3	0.25

Notes: E_B = Elastic modulus of slip bed; μ_B = Poison's ratio of slip bed; c_B = Cohesion of slip bed; φ_B = Internal friction angel of slip bed; E_M = Elastic modulus of slip mass; μ_M = Poison's ratio of slip mass; c_M = Cohesion of slip mass; φ_M = Internal friction angel of slip mass; E_Z = Elastic modulus of slip zone; μ_Z = Poison's ratio of slip zone.

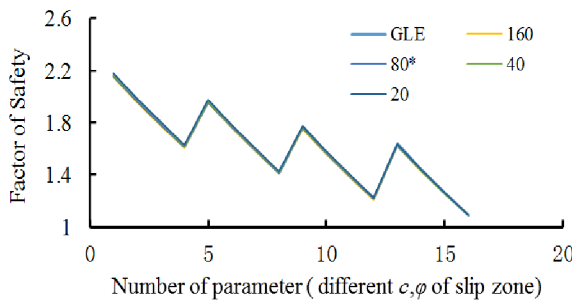

Figure 4 The result series.

Table 3 The Calculated Result Example

Parameter of Slip Zone			Local safety factor				
No.	c	φ	Elastic modulus of slip mass (MPa)				GLE
	(kPa)	(°)	160	80*	40	20	
1	65	32	2.150	2.158	2.167	2.176	2.165
2		28*	1.957	1.964	1.974	1.982	1.966
3		24	1.778	1.785	1.794	1.802	1.786
4		20	1.611	1.616	1.626	1.633	1.617
5	50*	32	1.952	1.958	1.966	1.974	1.969
6		28*	1.759	1.765	1.772	1.780	1.773
7		24	1.580	1.585	1.593	1.600	1.589
8		20	1.412	1.417	1.424	1.430	1.419
9	35	32	1.753	1.758	1.766	1.771	1.774
10		28*	1.560	1.565	1.571	1.576	1.577
11		24	1.381	1.385	1.391	1.396	1.395
12		20	1.210	1.217	1.222	1.227	1.221
13	25	32	1.621	1.626	1.633	1.639	1.644
14		28*	1.428	1.432	1.438	1.443	1.447
15		24	1.255	1.255	1.257	1.262	1.265
16		20	1.095	1.093	1.095	1.097	1.093

Table 4 Correlation Coefficient of Result Serials by Two Methods

No.	Parameter	Correlation coefficient			
		Value lever			
		1	2	3	4
1	E_B (MPa)	0.999639	0.999801	0.999900	0.999976
2	μ_B	0.999798	0.999791	0.999801	0.999799
3	c_B (kPa)	0.999801	0.999435	0.998751	0.998183
4	φ_B (°)	0.999801	0.999651	0.999073	0.998910
5	E_M (MPa)	0.999796	0.999801	0.999757	0.999723
6	μ_M	0.999837	0.999801	0.999818	0.999876
7	c_M (kPa)	0.999798	0.999797	0.999796	0.988048
8	φ_M (°)	0.999798	0.999799	0.999794	0.999780
9	E_Z (MPa)	0.999907	0.999853	0.999801	0.999654
10	μ_Z	0.999895	0.999801	0.999756	0.999699

4 Case History: Three-dimensional Stability and Sliding Mechanism

4.1 Numerical model

The Zhangjiaping Landslide is located in the town of Fenshui of the Wanzhou County and the town of Qushui of the Liangpin County along the Wan-Liang highway, along the segment of K34+817.2 -K34+922.4. The height of the landslide is 79.8 m, and the width is 118.2 m. The length of the landslide measured along the sliding direction is 262.6 m. The maximum thickness of the sliding mass is 29.7 m. (Figure 5 and Figure 6). The main body (slip body) of the landslide is comprised of colluvial deposits and diluvial deposits, which include weathering clast of shale and mudstone, gravelly soil and rock block. Slip bed is mainly composed of mudstone and shale. The weathering of rock mass is intense, and its structure is fractured. The soft soil from tense weathering product of mudstone and shale constitutes slip zone. Underlain the slip body, the slip zone is comprised of sandstone and sandy mudstone with interlayers of shale, which is highly weathered and fractured. The main scarp is obvious, so the head of the landslide is a step-like landform. And deformations occurred along both lateral boundaries of the landslide. However, the front part of the slope is stable without too much deformation, which indicates that the front part is more stable than the rear part (Figure 7(a)). From the geomorphological features analysis and geological field investigation, the Zhangjiaping Landslide is identified as an old landslide which occurred several decades ago. The slip surface is determined as shown in Figure 6. With the field observations, a physical model is made by available software as shown in Figure 7(b). The finite element discretization of the slip zone by eight node hexahedron elements with a thickness of 0.2 m and a length of 2 m is shown in Figure8(a). The mesh of the sliding mass and sliding bed is shown in Figure 8(b). The positions of the three slices (PX1、PX2、PX3) of slip surface along the transverse direction and other three slices (PY1、PY2、PY3) of slip surface along the longitudinal direction are shown in Figure 8(c). The transverse profiles of the slip surface are shown in Figure 8(d), the profiles on both sides (PY1 and PY3) are higher than the middle profile especially at the rear part of the slip surface. The longitudinal profile of the slip surface is shown in Figure 8(e), which shows a steep rear part, flat front part, and a linear middle part.

The values of parameters used in the calculations are shown in Table 5.

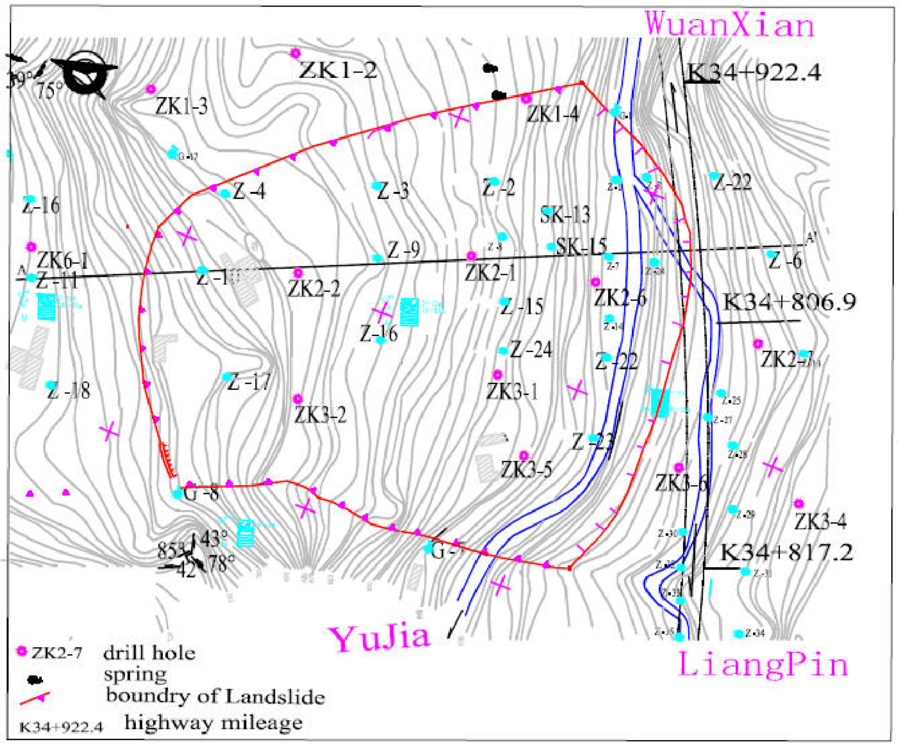

Figure 5 Engineering geological map of the Zhangjiaping landslide area.

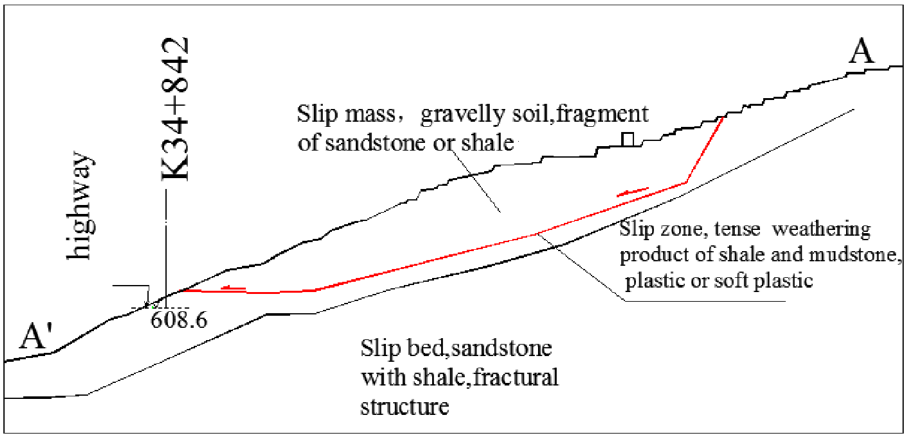

Figure 6 Section AA' along the main sliding direction.

Table 5 Calculation parameter

Rock Mass	E(MPa)	μ	c(kPa)	φ(°)	γ/(kN/m³)
Slip mass	80	0.3	120	20	20
Slip zone	30	0.35	35	25	18
Slip bed	1000	0.25	400	38	21

Notes: E = Elastic modulus; μ = Poison's ratio; c = Cohesion; φ = Internal friction angel; γ = Unit weight.

4.2 Stability of slope

The global safety factor of the slope is 1.139, as calculated by Eq.(15). The displacement vector along the slip surface and local safety factor distribution are shown in Figure 9. It can be seen from Figure 9 that the displacement vectors are not along the same direction. The displacement vectors in the slip surface are mostly along the main sliding direction. So the sliding direction is not uniform at the slip surface. Therefore, the shearing strength direction is not the same for every point when calculating the local safety factor.

The distribution of the local safety factor matches the slip surface, as shown in Figure 9(a). The distribution of local safety factor can be divided into three parts, the rear of the slip surface with a local safety factor lower than 1.05, which can be called the active zone, and where some scarps were observed in the field. The toe of the slip surface with a local safety factor larger than 1.10 can be called the passive zone, which is stable and providing support of the active zone. The middle part of the slip surface with a local safety factor ranging from 1.05 to 1.10 can be called the main sliding zone, which is at limit equilibrium, where field observations indicate that both sides of the slope had deformations.

To compare with other calculation methods, the local safety factor based on the Mohr-coulomb failure criterion (calculated by Eq.2) is shown in

(a) Field observation

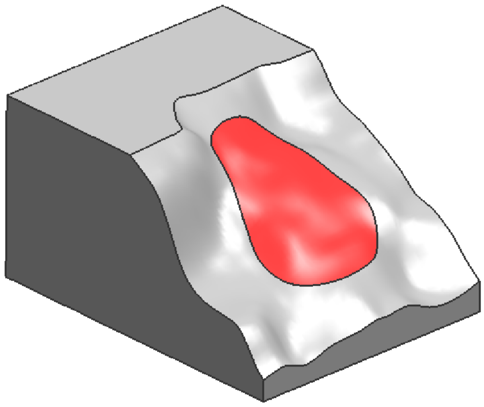

(b) Physical model

Figure 7 Geometric model of Zhangjiaping landslide.

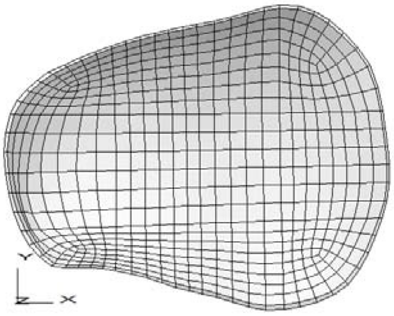

(a) Meshing of slip zone

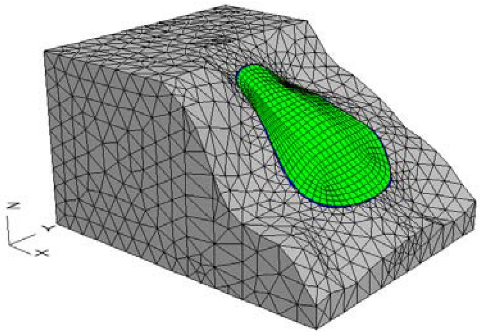

(b) Meshing of the slope

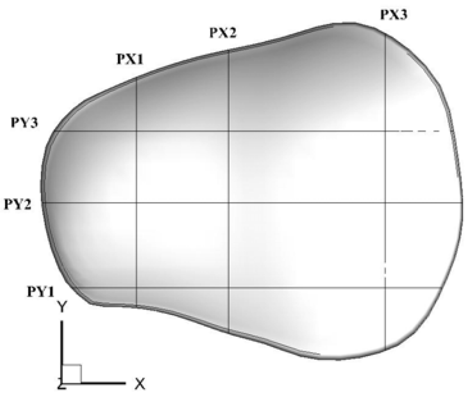

(c) Sections for slip zone

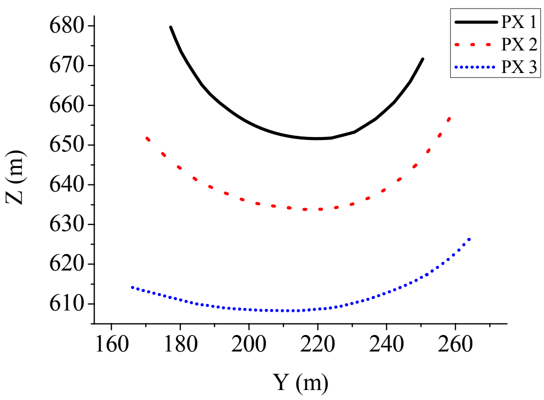

(d) Transverse sections

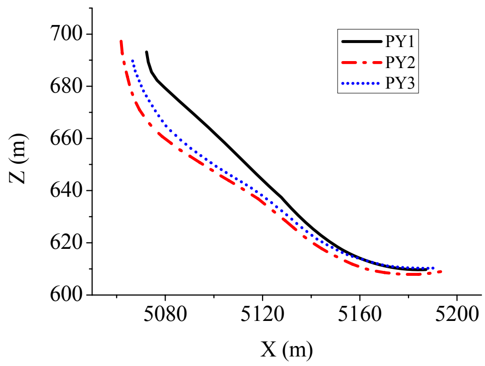

(e) Longitudinal sections

Figure 8 Computational mesh of Zhangjiaping landslide.

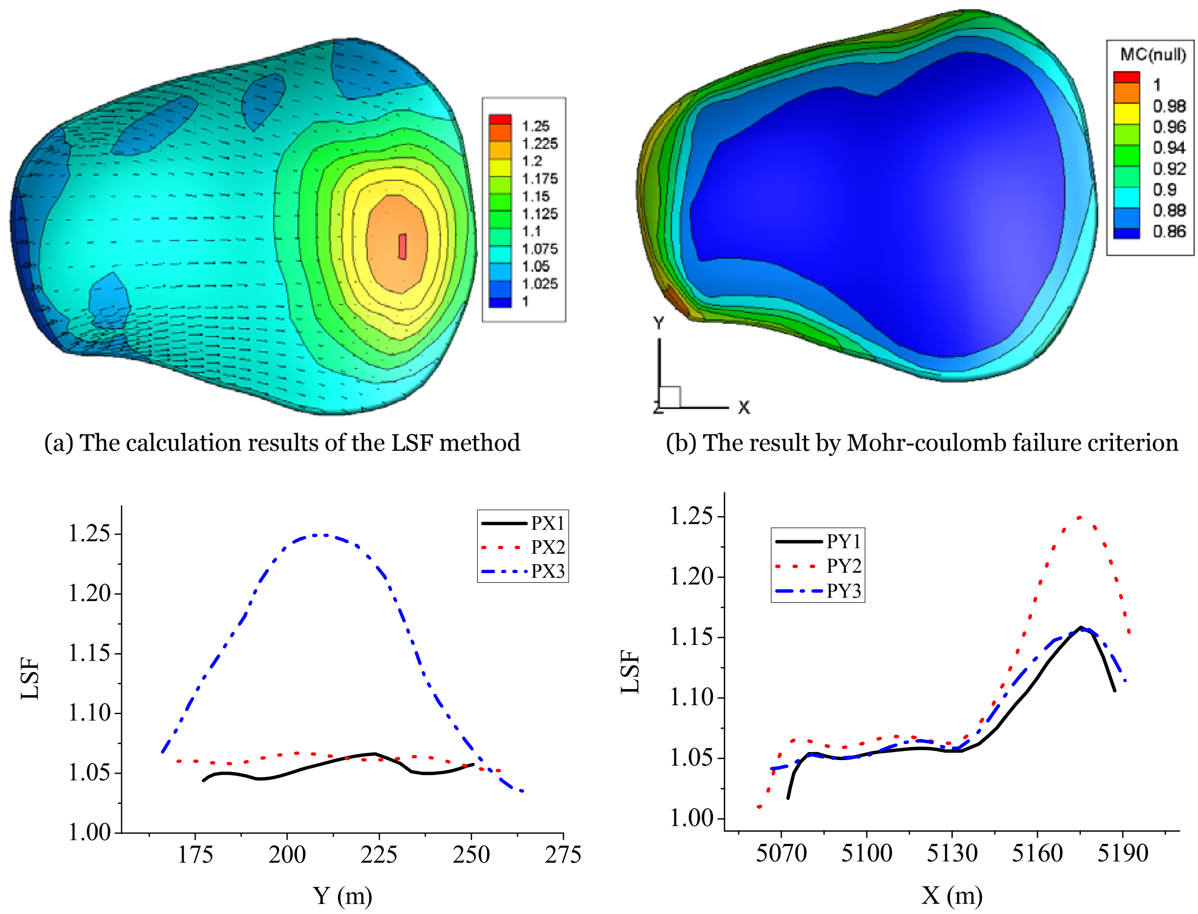

(a) The calculation results of the LSF method (b) The result by Mohr-coulomb failure criterion

(c) transverse distribution of local safety factor (d) longitudinal distribution of local safety factor

Figure 9 Distribution of local safety factor along the sections.

Figure 9(b). As an element in the slip zone yields to become plastic, the local safety factor will be close to 1.0. It can be seen from Figure 9(b), almost all the local safety factor of the slip surface is around 1.0. In this case the stability of different parts cannot be identified so that the sliding mechanism cannot be analyzed. Therefore, the local safety factor method simply based on strength criterion is inappropriate for sliding mechanism analysis. So, the actual slip surface and the slip direction must be taken into account.

Making a local safety factor distribution section along the transverse direction as shown in Figure 9, the local safety factor ranges from 1.05 to 1.10 and changes very little along sections PX1 and PX2. The curve is gentle and indicates that the part of the slip surface in the section is at limit equilibrium. For the section PX3, the local safety factor is relatively large in the middle part while that of the both sides approaches 1.0, indicating that both sides of the section have a lower stability and that the middle of the section provides passive support forces. When making section along the longitudinal direction as shown in Figure 8(c), the distributions of the local safety factor on these three sections have the same characteristics: the crest of the section is unstable with a local safety factor smaller than 1.05; the middle of the slice is at limit equilibrium with a local safety factor ranging from 1.05 to 1.10; and the toe of the section provides passive supporting forces with a local safety factor larger than 1.10. This is obvious when looking at section PY2 in Figure 9(d).

5 Conclusion

In this paper, a novel method, i.e. the local safety factor method (LSF), is proposed to evaluate the stability of a landslide. In the numerical analysis, the material of the slip zone is selected as the ideal elastic-plastic model and the Mohr-Coulomb yield criterion is adopted. The slip zone is discretized into many small eight-node hexahedral elements. The local safety factor is defined on the single element. The local safety factor is defined as the ratio of the shear strength of the soil at an element on the slip zone to the shear stress parallel to the sliding direction at that element. The shear stress parallel to the sliding direction at an element on the slip zone is obtained through 3D numerical simulation, and the shear strength of the soil at an element on the slip zone is computed according to the Mohr-Coulomb theory. The LSF method gives the stability factor of every point on the slip surface. The global safety factor is determined through the area-weighted average of the local safety factors on the slip surface.

A 2D slope model is adopted to verify the reliability of the LSF method. The results computed by the LSF and GLE methods are compared. It was found that the two methods agree well with each other for the analysis of two-dimensional slope models.

This LSF method is applied to analyze the stability of a landslide located at Wan-Liang highway in China. The local safety factor of the slip zone is calculated. The distribution of local safety factor can be divided into three regions, i.e. an active zone, a main sliding zone, and a passive zone, and the stability indicated by distribution of the LSF was consistent with that indicated by the deformations observed in the field.

The local safety factor method in this paper not only can be used to evaluate the global stability of landslides, it also can be used to analyze the failure mechanism of the landslide. Based on the distribution of the local safety factor, rational landslide mitigation measures can be designed, and the real shear strengths of the slip zone can be back calculated.

Acknowledgements

This work was financially supported by the National Natural Science Foundation of China (Grant No. 51178402, 10902112), Department of Transportation Technology Projects (Grant No. 2011318740240) and the Fundamental Research Funds for the Central Universities (Grant No. 2682014CX074).

References

Alemdag S, Akgun A, Kaya A, et al. (2014) A large and rapid planar failure: causes, mechanism, and consequences (Mordut, Gumushane, Turkey). Arabian Journal of Geosciences 7: 1205-21. DOI: 10.1007/s12517-012-0821-1

Alemdag S, Ayberk K, Mustafa K, et al. (2015) Utilization of the limit equilibrium and finite element methods for the stability analysis of the slope debris: An example of the Kalebasi District (NE Turkey). Journal of African Earth Sciences 106: 134-146. DOI: 10.1016/j.jafrearsci.2015.03.010

Anagnosti P (1969) Three-dimensional stability of fill dams. In: Proceedings 7th international conference on soil mechanics and Foundation Engineering, Mexico City, 1969, vol. 2, pp 275-280.

Baker R (1980) Determination of the critical slip surface in slope stability computations. International Journal for Numerical and Analytical Methods in Geomechanics 4(4): 333-359.

Baligh MM, Azzouz AS (1982) End effects on stability of cohesive slopes. Journal of Geotechnical Engineering Division (ASCE) 101(11): 1105-1117.

Chen RH, Chameau JL (1982) Three-dimensional limit equilibrium analysis of slopes. Geotechnique 33(1): 31-40.

Duncan JM (1996) Limit equilibrium and finite element analysis of slopes. Journal of geotechnical engineering 17(122): 577-596. DOI: 10.1061/(ASCE)0733-9410(1996)122:7(577)

Fairhurst C (1964) On the validity of the brazilian test for brittle materials. International Journal of Rock Mechanics and Mining Science 1(1): 535-546.

FLAC-3D (2005) User's Guide: fast Lagrangian analysis of continua in 3 dimensions-version 3.0. Itasca Consulting Group Inc, Minnesota, USA.

Hoek E, Bray J (1981) Rock slope engineering. Institute of Mineral and Metallurgy, London, UK.

Huang CC, Tsai CC, Chen YH (2002) Generalized method for three-dimensional slope stability analysis. Journal of Geotechnical and Geoenvironmental Engineering 128(10): 836-848. DOI: 10.1061/(ASCE)1090-0241(2002)128:10(836)

Hutchinson JN (1982) Methods of locating slip surface in landslides. British Geomorphological Research Group, London, UK.

Jaeger C (1965) The Vajont rock slide. Water Power 4(17): 142-144.

Jaiswal P, Cees JW, Victor J (2011) Quantitative assessment of landslide hazard along transportation lines using historical records. Landslides 8: 279-91. DOI: 10.1007/s10346-011-0252-1

Kahatadeniya KS, Pruettha N, Krishna MN (2009) Determination of the critical failure surface for slope stability analysis using ant colony optimization. Engineering Geology 108: 133-41. DOI: 10.1016/j.enggeo.2009.06.010

Krahn J (2003) The limits of limit equilibrium analyses. Canadian geotechnical journal 40: 643-660. DOI: 10.1139/T03-024

Kaya A, Alemdag S, Dag S et al. (2016) Stability assessment of

high-steep cut slope debris on a landslide (Gumushane, NE Turkey). Bulletin of Engineering Geology and the Environment 75: 89-99. DOI: 10.1007/s10064-015-0753-6
Leshchinsky D, Huang CC (1992) Generalized three-dimensional slope-stability analysis. Journal of Geotechnical Engineering (ASCE) 118(11): 1748-1764.
Mankelow JM, Murphy W (1998) Using GIS in the probabilistic assessment of earthquake triggered landslide hazards. Journal of Earthquake Engineering 2(4): 593-623.
Colomer MFJ, Gisbert AF, Izquierdo AG, et al. (2009) Safety factor nomograms for homogeneous earth dams less than ten meters high. Engineering Geology 105: 231-38. DOI: 10.1016/j.enggeo.2009.01.001
Morgenstern NR, Price VE (1965) The analysis of the stability of general slip surfaces. Geotechnique 1(15): 79-93.
Morgenstern NR, Price VE (1967) A numerical method for solving the equations of stability of general slip surfaces. The Computer Journal 9: 388-93.
Nguyen V (1985) Determination of critical slope failure surfaces. Journal of Geotechnical Engineering 111(2): 238-250.
Okubo S, Fukui K, Nishimatsu Y (1997) Local safety factor applicable to wide range of failure criteria. Rock Mechanics and Rock Engineering 30(4): 223-227. DOI: 10.1007/BF01045718
Ono K (1962) On the load of materials. Transactions of Society of Materials Engineering 16(29): 37-48.
Ozbay A, Cabalar AF (2015) FEM and LEM stability analyses of the fatal landslides at Collolar open-cast lignite mine in Elbistan, Turkey. Landslides 12:155-163. DOI: 10.1007/s10346-014-0537-2
Irons BM (1971) Quadrature rules for brick based finite elements. International Journal for numerical methods in Engineering, 3: 293-294.
Srbulov M (1987) Limit equilibrium method with local factors of safety for slope stability. Canadian Geotechnical Journal 24(4): 652-656.
Van Westen CJ (1994) GIS in landslide hazard zonation: a review, with examples from the Andes of Colombia. In: Price MF, Heywood DI (Eds.), Mountain Environments & Geographic Information Systems, Chapter: GIS in Landslide Hazard Zonation: A Review, with Examples from the Andes of Colombia. Publisher: Taylor and Francis, pp.135-166.
Wang LT, Zhou WH (1982) Stability analysis of rockmass at the Arc Dam Abutment. Guizhou People Press, Guiyang, China.
Werner ED, Friedman HP (2009) Landslides: Causes, Types and Effects. Nova Science Publishers, New York, USA.
Xu JC (2011) Debris slope stability analysis using three-dimensional finite element method based on maximum shear stress theory. Environmental Earth Sciences 64: 2215-22. DOI: 10.1007/s12665-011-1049-1
Yao BK, Sun YK, Liu ZH (1984) Stability analysis of slip mass in slopes under the geotechnical stress. Metal mine 4: 16-20.
Zheng H (2012) A three-dimensional rigorous method for stability analysis of landslides. Engineering Geology 145-146: 30-40. DOI: 10.1016/j.enggeo.2012.06.010